

Received 13 February 2024, accepted 7 March 2024, date of publication 13 March 2024, date of current version 2 May 2024.

Digital Object Identifier 10.1109/ACCESS.2024.3376753

## RESEARCH ARTICLE

# Pneumatically Controlled Wearable Tactile Actuator for Multi-Modal Haptic Feedback

AHSAN RAZA<sup>1</sup>, WASEEM HASSAN<sup>2</sup>, AND SEOKHEE JEON<sup>1</sup>, (Member, IEEE)

<sup>1</sup>Department of Computer Engineering, Kyung Hee University, Yongin, Gyeonggi 17104, South Korea

<sup>2</sup>Department of Computer Science, University of Copenhagen, 1356 Copenhagen, Denmark

Corresponding author: Seokhee Jeon (jeon@khu.ac.kr)

This work was supported in part by the Ministry of Science and Information and Communications Technology (ICT) Korea under the Information Technology Research Center (ITRC) Support Program Supervised by Institute for Information & communication Technology Planning & evaluation (IITP) under Grant IITP-2023-RS-2022-00156354, in part by IITP Program Supervised by IITP under Grant 2022-0-01005, and in part by the Mid-Researcher Program Supervised by the NRF Korea under Grant 2022R1A2C1008483.

This work involved human subjects or animals in its research. Approval of all ethical and experimental procedures and protocols was granted by the Kyung Hee University Institution Review Board.

**ABSTRACT** This paper introduces a wearable pneumatic actuator, designed for providing multiple types of tactile feedback using a single end-effector. To this end, the actuator combines a 3D-printed framework consisting of five 0.5 DOF soft silicon air cells with a pneumatic system to deliver a range of tactile sensations through a single end-effector. The actuator is capable of producing diverse haptic feedback, including vibration, pressure, impact, and lateral force, controlled by an array of solenoid valves. The design's focus on multimodality in a compact and lightweight form factor makes it highly suitable for wearable applications. It can produce a maximum static force of 8.3 N, vibrations with an acceleration of up to 3.15 g, and lateral forces of up to 3.3 N. The efficacy of the actuator is demonstrated through two distinct user studies: one focusing on perception, where users differentiated between lateral cues and vibration frequencies, and another within a first-person shooter gaming scenario, revealing enhanced user engagement and experience. The actuator's adaptability to body sites and rich multimodal haptic feedback enables it to find applications in virtual reality, gaming, training simulations, and more.

**INDEX TERMS** Multimodal tactile feedback, pneumatic, vibrotactile, pressure, haptic actuator.

## I. INTRODUCTION

Haptic feedback holds significant importance in shaping interactive experiences, including Virtual Reality (VR) environments [1], [2]. Haptic feedback can be broadly categorized into two primary forms: tactile feedback and kinesthetic feedback [3]. Kinesthetic feedback relies on devices that engage users' joints, muscles, and tendons, enabling them to perceive positional changes through force feedback [4]. On the other hand, tactile feedback focuses on the skin's ability to perceive haptic properties, such as vibrations and pressure, during interactions. While both tactile and kinesthetic feedback play crucial roles in haptic interactions, the current research is

The associate editor coordinating the review of this manuscript and approving it for publication was Lei Wei<sup>1</sup>.

dedicated to understanding the capabilities of tactile feedback across multiple tactile modalities and exploring its potential in various applications, including wearable technology.

Numerous studies have focused on providing rich tactile feedback, achieving considerable success in delivering a realistic and immersive user experience. Tactile feedback technology evolves towards wearable modes of actuation for better usability and accessibility. However, wearable tactile feedback devices have mostly been constructed around a single type of actuator, which limits them to providing only a specific form of haptic signal. As the demands of modern VR technologies intensify, there is an increasing need for diverse tactile signals at the same time to ensure enriched user engagement. For instance, when simulating scenarios where debris strikes a body site, the ideal tactile

sensation should encompass various aspects, such as impact, vibration, and directional cues. Nevertheless, achieving such intricate sensations becomes challenging with a single form of actuation.

To achieve multiple signal generation through a single device, one potential solution is to integrate multiple single-feedback actuation modules to achieve various forms of feedback [5]. However, integrating multiple actuators on a small sensitive skin area is not straightforward, as it makes delivering spatially and temporally concurrent and concentric actuation difficult. Moreover, such a setup can become bulky and less practical for wearable applications. This has led recent research to pivot towards devising methods that can convey multi-modal feedback via a single actuation principle and through a single end-effector [3].

Research in multi-modal haptic devices initially centred on the fingertips due to their superior sensitivity and frequent engagement in tactile interactions [6]. This strategy subsequently expanded to explore multi-modal feedback capabilities for other body parts [7], [8]. Notably, many of these devices are specifically designed for certain body sites, raising concerns about their overall effectiveness and practicality in real-world applications. Achieving a balance between compactness, providing multi-mode feedback, and usability continues to be a significant challenge in the domain of wearable haptic technology. As a result, there's an evident gap and consequent need to develop designs that not only deliver robust multi-modal feedback but also demonstrate versatility across various body sites. Addressing this gap could significantly improve user experience and expand the applications of haptic devices.

This research presents a novel design of a wearable pneumatic actuator capable of delivering diverse forms of tactile signals through a single actuator with a single end-effector. The actuator features a 3D-printed model containing 5 air chambers. Each air chamber is covered with a soft silicon inflatable air cell, capable of delivering strong and fast 0.5 DOF (degree of freedom) movement. The five chambers are arranged so that they can deliver 2.5 DOF feedback to the end-effector. With this design, the actuator can provide a multitude of tactile feedback including vibration (normal and lateral), static pressure, impact, and lateral force cues in 2.5 DOF. The actuator achieved a high static pressure of 8.3 N as well as successfully generated a vibration with an acceleration of 3.15g at 10 psi. Of particular interest is the device's ability to produce lateral force actuation up to 3.3 N, which is a feature less commonly observed in similar designs. This addition enhances the device's ability to simulate sliding or shear force feedback, enriching the spectrum of haptic experiences it offers. Another feature of the device's design is its adaptability to different body locations. Using a velcro strap, it can be easily affixed around various body parts, including the arm, wrist, and leg, facilitating straightforward wearability.

To highlight the significance and advancement of our work, we outline the principal contributions as follows:

- Introduced a wearable pneumatic actuator with a 3D-printed model featuring 5 air chambers, enabling diverse tactile signals through a single end-effector
- The device can provide a concurrent multimodal tactile sensation to enable complex haptic feedback.
- Achieved significant performance with high static pressure and vibration acceleration, demonstrating the device's capabilities.
- Designed for adaptability, the device can be easily attached to various body parts such as the arm, wrist, and leg, promoting ease of use in different contexts.

By addressing the limitations of single-form actuation and existing multi-modal devices, this research seeks to contribute to advancing haptic technology, opening up possibilities for more immersive and realistic interactions.

The rest of the article is organized as follows. Section II provides an overview of the literature related to wearable devices and multimodal feedback systems. Section III and IV contain the complete information regarding the actuator design and fabrication methodology respectively. Section V explains the control mechanism in the light of some key example scenarios. Section VI provides details regarding the characterization of the actuation along with some results. Section VII and VIII explain the details of the user perception experience evaluation of the proposed actuator respectively. Section IX provides the general discussion about the proposed work. Section X concludes the overall work.

## II. RELATED WORKS

The proposed wearable multi-modal device is designed to provide diverse forms of tactile signals concurrently. In general, each tactile signal has unique characteristics and requirements to be produced by interfaces. In this section, we present the literature review to understand haptic technologies that provide three major tactile signals: vibrotactile, impact, and pressure signals. Then, the review covers efforts to provide multiple tactile signals.

### A. VIBROTACTILE ACTUATORS

Compactness and lightness are essential for a wearable haptic setup, as the intention is to affix it to a body segment. Vibrotactile feedback actuators typically possess a diminutive size and weight, making them ideal for integration into a portable/wearable environment. These actuators are typically based on electromagnetic principles. Within this category, two extensively utilized types are eccentric rotary mass (ERM) and linear resonant actuators (LRAs) [9], [10], [11], [12].

ERM actuators offer effective vibrotactile feedback. However, their actuation principle, which relies on DC motors, results in a lack of separate control over frequency and amplitude [13], [14]. In these actuators, the strength of

vibration amplitude is directly tied to the input voltage. On the contrary, LRAs provide the advantage of independent control over amplitude and frequency. Nonetheless, these actuators come with a trade-off, which includes a limited frequency bandwidth and residual vibrations after actuation [15].

Another category, distinct from electromagnetic mechanisms, relies on the piezoelectric phenomenon to generate vibrotactile actuators. Vibrations are induced through the piezo effect when a high input voltage is applied to ceramic or polymer materials [16], [17]. The upside of this approach is the ability to target a broader frequency bandwidth. Nonetheless, the downside is the necessity for a substantial input voltage to achieve the desired actuation, coupled with a notably low vibration amplitude [6].

While vibrotactile actuators have been widely used due to their simplicity and compactness, they are often limited to providing only a small number of effects since the form of vibration is relatively rarely observed in real physics.

### B. IMPACT/PRESSURE ACTUATORS

When discussing wearable haptic interfaces, numerous solutions are available that propose methods for delivering pressure feedback based on specific body sites, such as the hand/finger, wrist, arm and head. For instance, Biernacki et al. proposed a pressure feedback device that enables artists to understand the currently active musical effect and its strength [18]. Evan et al. present Tasbi, a bracelet designed for easy wear at the wrist, effectively enabling the presentation of normal squeeze force around the wrist [19], [20]. Kanjanapas et al. presented a pneumatically controlled 2-Dof haptic device capable of generating a shear force up to 1N [21]. The study shows the performance of shear force display and directional cues on the user's forearm. Some wearable devices are built by using a pair of servo motors and belts to generate pressure feedback on the user's forearms [22], [23]. Facepush and PneumoVolley are the solutions designed to be worn on the face to provide pressure feedback while interacting with objects in a VR environment [24], [25]. A common feature of these actuators is their single type of feedback and a firm reliance on specific body sites which limits their applicability.

### C. MULTI-MODE ACTUATORS

There have been a considerable number of efforts to provide multiple forms of actuation through a single device. These multi-mode devices encompass various actuation types such as vibration, force, pressure, and shear force, each of which contributes to a comprehensive haptic experience. Talhan et al. introduced a soft haptic tactile ring [6] and tactile thimble [26]. Both solutions leverage pneumatic systems to deliver distinct forms of feedback to human fingers. Another study presented by Zhakypov et al. proposed a 4-DOF haptic device for fingertip [27]. The device uses pneumatic actuation to generate pressure, linear and rotational shear, and vibration feedback on the user's fingertip. Kyle et al., through a combination of a pneumatic actuator and a DC motor,

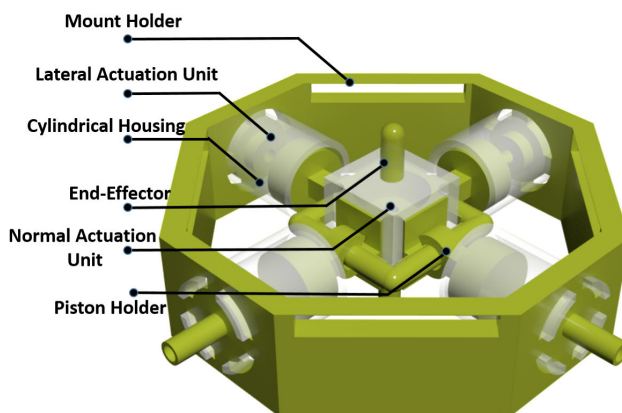


FIGURE 1. 3D Design of Pneumatically controlled Multi-Modal Tactile Actuator (MMTA).

proposed a 3-DOF wearable haptic device for the human forearm [7]. This device is capable of providing normal force, shear, and vibration sensations to the forearm. Additionally, another device named HaptGlove allows users to interact with virtual objects while perceiving multiple forms of feedback [8]. These multi-mode feedback devices mark a significant step towards enriching haptic experiences by offering a wider spectrum of tactile cues.

However, many multimodal actuators are designed for specific body parts, limiting their use in different scenarios. The pneumatic actuator proposed in this study overcomes this by being adaptable to different body sites offering greater usability and application potential. This adaptability is crucial for the wider implementation of haptic technology in diverse fields.

## III. CONCEPT AND DESIGN OF ACTUATOR

The proposed multimodal haptic device's foundation lies in several criteria essential for wearable haptic technology, such as wearability, usability, and the capacity to deliver strong multimodal feedback with a single end-effector. To incorporate the aforementioned criteria, the proposed device consists of three components; a 3D-printed design, a pneumatically-controlled actuation system, and a soft silicon air cell. This section explains how the proposed solution embodies these pivotal factors.

### A. HARDWARE DESIGN

The proposed multimodal haptic actuator is shown in Fig. 1. The multimodal actuator is designed to provide diverse feedback using a single end-effector. Its octagonal form houses five actuation points (APs), each covered with a soft silicon inflatable air cell. Four of these points are positioned at the edges of the octagonal body called the lateral actuation units (LAUs), while the fifth is located in the centre called the normal actuation unit (NAU). The LAUs are geared towards lateral-directional vibrations and force feedback, while the NAU is tailored for normal-directional vibrations and pressure feedback. The key design aspect in this assembly

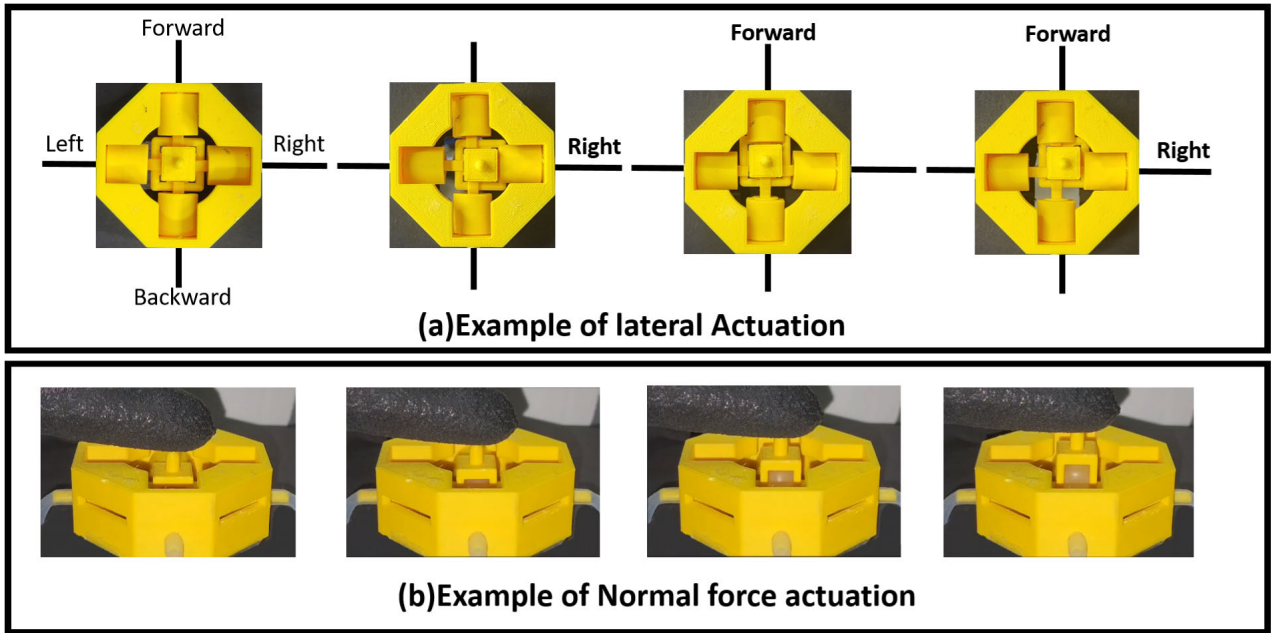


**FIGURE 2.** (a) Example of actuation in 2D area. The first picture on the left shows the actuator in its default state of no actuation, the second picture shows lateral motion to the right, the third picture shows actuation forward, and the rightmost picture shows right-forward actuation. (b) Example of actuation in the normal direction. The pictures from left to right show increasing normal force as the end-effector moves up.

is that the NAU is the only unit that establishes contact with the user during actuation. It gathers feedback from all other units, includes its normal feedback if required, and delivers it to the user. Such a design enables the deliverance of concurrent multimodal feedback using a single end-effector.

**B. PNEUMATIC SYSTEM**

Pneumatic actuation holds a prominent position in the field of wearable haptics for delivering haptic feedback [28]. The system’s inherent ability to produce substantial pressure levels and execute swift actuation changes establishes it as an effective haptic interface [29], [30], [31]. In the present study, we employ pneumatic actuation to establish a multimodal haptic feedback mechanism. This is facilitated by an air cartridge designed to supply pressurized air to the actuating device, managed by a pressure regulator. Considering the user’s mobility during wearable application scenarios, a 16-gram CO<sub>2</sub> cartridge would be sufficiently lightweight and portable, allowing for more freedom of movement [32]. It is estimated that such a cartridge can provide a steady air supply for up to an hour in typical interaction scenarios, as noted in [6]. We use electronically controlled solenoid valves, with a response time of 2 ms, to control the rapid pressure change. Figure 2(a) and 2(b) illustrate the example actuation caused by controlling the solenoid valves.

**C. SILICON AIR CELL**

Air from the source cartridge is channelled into specially designed chambers within the device. To facilitate accurate actuation, a design incorporating a soft silicon air cell is used to securely encase all the device’s internal air chambers. The fabrication of these silicon air cells employs Ecoflex

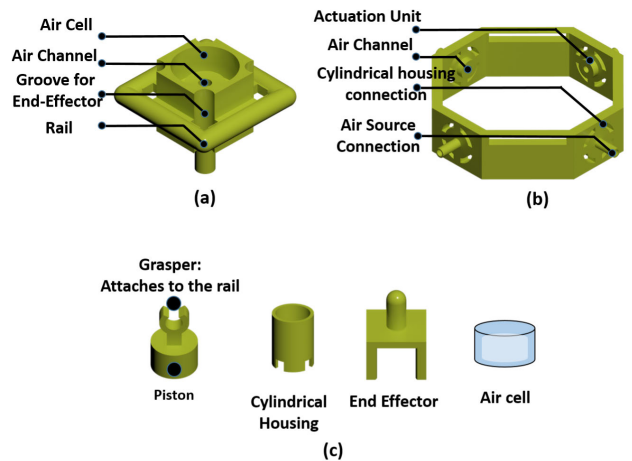


**FIGURE 3.** (a) Normal Actuation Unit (NAU), (b) Lateral Actuation Unit (LAU), (c) Components used to form the complete actuator.

00-30(Smooth-on, Inc.). This material, with its resilience and elasticity, has previously proven beneficial in the domain of pneumatic-based haptic feedback mechanisms. Figure 3 (c) illustrates the design of the air cell.

**IV. FABRICATION PROCEDURE**

The creation of the multimodal actuator involved a two-phase fabrication process. The first phase involved 3D printing the components required for the device. The subsequent phase focused on the creation of soft silicon inflatable air cells. The procedures for each are detailed below.

**A. 3D MODELING AND PRINTING**

The two main components of the design are the NAU and the LAUs. Their details are provided below.

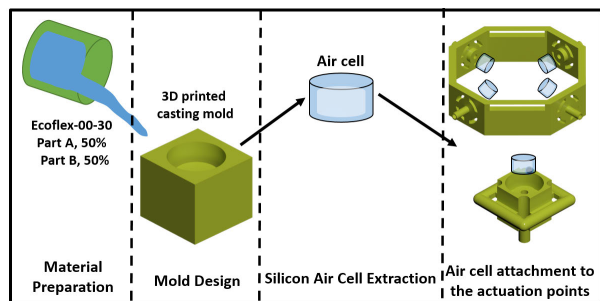


FIGURE 4. Fabrication procedure of the air cell.

### 1) NORMAL ACTUATION UNIT (NAU)

This unit adopts a cubical form, further augmented with a rail-like structure that extends from its sides as shown in Fig. 3(a). A cylindrical groove, with dimensions of 6 mm in diameter and 5 mm in height, was incorporated to house the air. An air channel, attached to this cavity, ensures a steady flow of air from the inlet valves.

### 2) LATERAL ACTUATION UNIT (LAU)

This unit is distinguished by its octagonal form. Four of its sides house the APs, each of which is connected to air channels, mirroring the configuration explained above (Fig. 3(b)).

While both the NAU and LAU have independent actuation capabilities, they can be connected for integrated feedback. To achieve this, supplementary components were designed and 3D printed: a cylindrical housing, a piston-shaped holder, and an end effector. The cylindrical housing is aligned with the four LAUs and directs the pneumatic actuation in a linear path. The piston-shaped holder slides along the rails of the NAU and operates within the confines of the cylindrical housing. This mechanism ensures that the initiation of pneumatic actuation transmits motion feedback to the piston holder, which in turn transmits linear motion to the NAU. The end effector serves to convey feedback to the user. Its design allows for smooth movement along the corners of the NAU, making it responsive during normal actuation and stable during lateral actuation. Fig. 3(c) presents the remaining component designs.

The complete set of components was produced using a Zortrax M200 3D printer, utilizing ABS plastic as the fabrication material.

## B. FABRICATION OF THE INFLATABLE AIR CELL

This air cell is tailored to fit the cylindrical groove in the NAU and LAUs. The fabrication is carried out in a series of steps. The following sections explain each step in detail.

### 1) MOLD DESIGN

A casting mold was crafted using the 3D printer. This mold aimed to ensure the air cell's dimensions were ideal for compatibility with both the NAU and the LAUs. The mold's 3D model and its integration with NAU and LAUs are depicted in Fig. 4.

### 2) MATERIAL PREPARATION AND AIR CELL FORMATION

To fashion the stretchable silicon air cell, we employed Ecoflex 00-30 (Smooth-on, Inc., Young's modulus of 0.1694 Mpa at 10 Psi). This material comprises two components: Parts A and B. These were amalgamated in equal measures. Once the components were thoroughly mixed, the resultant material was decanted into the casting molds for NAU and LAUs. These were then left to set for approximately 4 to 5 hours, to form the stretchable silicon air cells.

### 3) INTEGRATION OF AIR CELLS

Once set, the silicon air cells were gently taken out from their molds and glued to each actuation point. This ensured the air chamber was entirely enveloped by the silicon air cell, creating the ideal environment to generate pressure upon inflation. The detailed procedure, starting from the fabrication of the air cell to its attachment with the 3D printed components, resulting in the creation of the multimodal pneumatic actuator, is showcased in Fig. 4.

## V. CONTROL MECHANISM

The actuator's haptic feedback is primarily driven by modulating the air pressure within the air chamber at the actuation points. Two DC micro solenoid valves (Fspump, Model: 0520D, Voltage: 6V) are integrated into each AP. These are the positive valve, which controls air inflation, and the negative valve, responsible for air deflation.

Each valve is conjoined to a 2-to-1 Y-shaped hose connector in parallel. The opposite end of this connector attaches directly to the AP. The air source engages one end of the positive valve, with its other end being connected to the AP via the Y-shaped connector. One end of the negative valve links to the AP, drawing air from the chamber and releasing it into the environment through the other end, which reduces the chamber's pressure. The overall pneumatic actuation control system is illustrated in Fig. 5

To cater to the five APs, a total of 10 solenoid valves (comprising five positive and five negative valves) were used. Given the digital controllability of these valves, a custom circuit board with MOSFET transistors is designed according to instructions given in [33] This board acts as an intermediary between the input channels of the microcontroller (Arduino Uno board) and the solenoid valves. The input channels send 'on' and 'off' commands to each solenoid valve, facilitating precise control. The valve control unit is illustrated as a block in Fig. 5.

Various control strategies have been employed to yield specific haptic effects using the proposed multimodal haptic actuator explained as follows.

### 1) VIBRATION CONTROL

Each actuation point's paired positive and negative valves enable either normal or lateral vibration control. The method

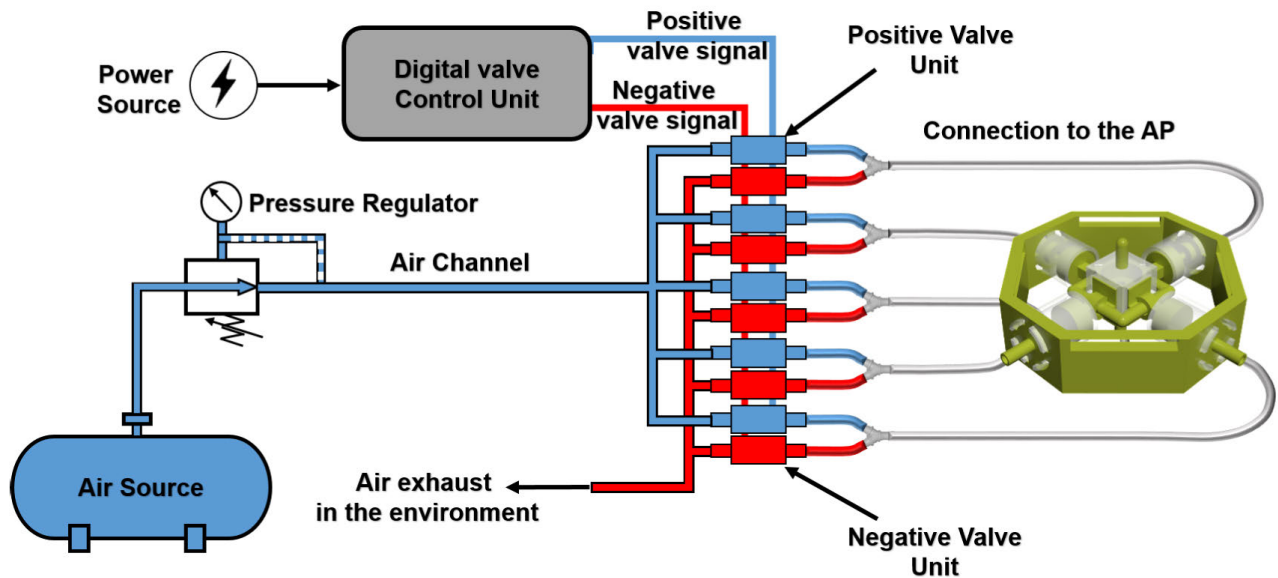


FIGURE 5. Pneumatic actuation control system.

initiates by briefly opening the positive valve and then closing it. Once the chamber is saturated with air, the negative valve is opened and closed to evacuate the chamber's air. This cycle, when perpetually executed, simulates a vibration sensation. By modulating the valve's opening span and duty cycle, the vibration's frequency and amplitude can be adjusted. Fig. 6(a, b) depicts this vibration control approach for rendering a signal with a 50 Hz frequency.

## 2) PRESSURE AND IMPACT FEEDBACK CONTROL

The silicon air cell retains pressures up to 10 psi. Two distinct pressure effects can be generated. The first, termed static pressure, involves a sustained opening of the positive valve, followed by its closure, entrapping air and establishing a consistent pressure effect. By subsequently opening the negative valve, the chamber's pressure is reduced, reverting the actuator to its primary state. Fig. 6(c) illustrates an example of valve control for pressure feedback.

The second method, called impact feedback, is realized by swiftly opening the positive valve, followed by its closure and the immediate opening of the negative valve, rendering an instantaneous impact sensation. Fig. 6(d) illustrates the control mechanism for impact feedback.

## 3) LATERAL MOTION AND POSITION CONTROL

Lateral motion control capitalizes on the four APs. Unique movement patterns can be derived either by singular actuation point control or a combined approach. For instance, to initiate a leftward signal, the right actuation point's valve is activated. Compound motions, such as diagonally, necessitate synchronized control of multiple APs. This is explained in Fig. 6(e).

Position control requires the synchronized operation of two APs. If the end effector has to traverse a short forward distance, the valves of both the back and front APs must be activated sequentially, with a time interval between

activations. The rear valve must be activated first for a set duration, propelling the end effector forward. Subsequently, the forward actuation valve activates as resistance and halts the end effector at a designated location. This control mechanism is illustrated in Fig. 6(f). It is to be noted that the percentage values in 6(f) are shown as a reference to understand valve state control duration for a pair of valves involved in position control.

## 4) MULTIMODAL FEEDBACK CONTROL

The integrated digital control unit is designed to issue commands that target each AP independently. This intricate level of control provides the user with the capability to produce the activation of several APs concurrently, creating a rich multimodal feedback experience. Consider a scenario where a user desires to produce a specific haptic effect that combines both normal pressure and lateral vibrations. In such a case, by harnessing the control mechanisms illustrated in Fig. 6(b) and 6(c), the intended synchronized action can be adeptly achieved.

## VI. CHARACTERIZATION OF ACTUATION MODES

The primary actuation modes of the device are examined by conducting a series of measurement experiments. Separate measurement setups are designed for each actuation mode. The following subsections detail each actuation mode.

### A. VIBRATION FEEDBACK MEASUREMENT

The device can render vibration feedback in both normal and lateral directions. The valve control mechanism, shown in Fig. 6(2), explains an example of a valve control setup to render vibration with a specific frequency. The acceleration response of the rendered vibrations was measured under the combination of different pressure levels and vibration frequencies.

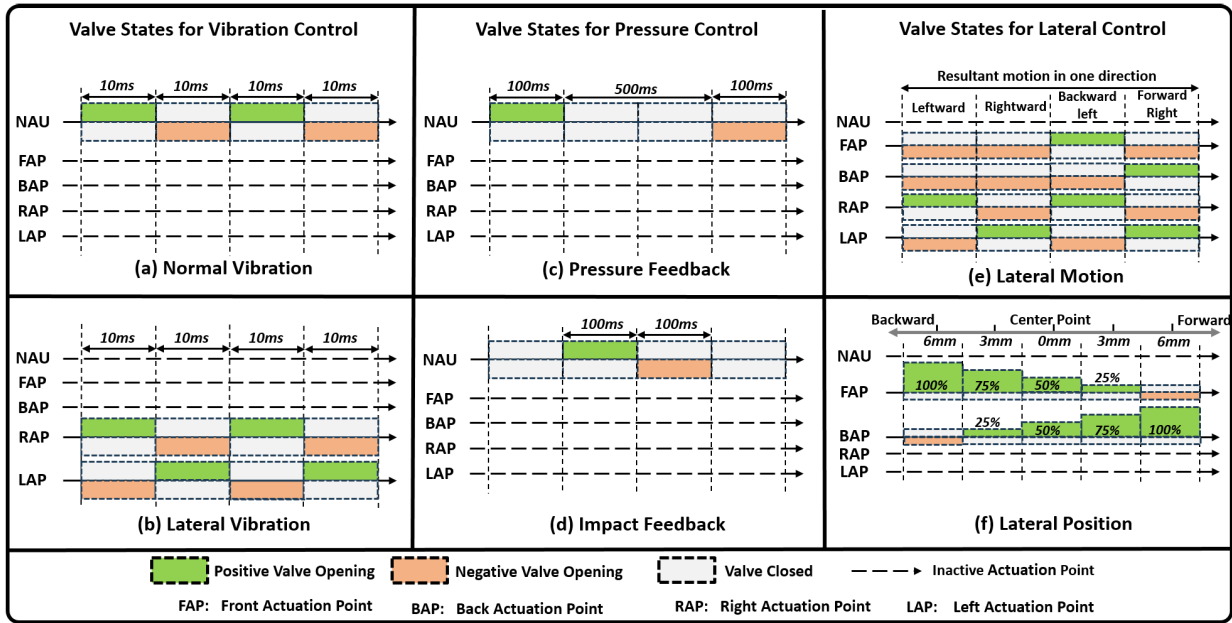


FIGURE 6. Valve control mechanism to produce different modes of actuation.

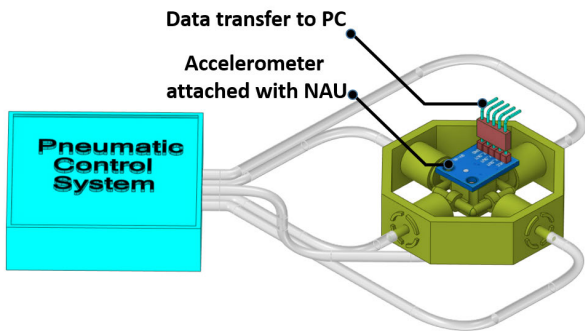


FIGURE 7. Acceleration measurement setup.

1) MEASUREMENT PROCEDURE

To measure the acceleration response from the actuation, the accelerometer, ADXL335 GY-61, was attached to the NAU (illustrated in Fig. 7). The acceleration data was recorded using a data acquisition unit (NI-DAQ 6009), and Matlab was used to store the data on the PC. During measurement, the vibration frequency ranged from 1Hz to 250 Hz with a gradual increase in the step sizes of frequency to analyze the response. In addition, each frequency level was commanded at 3 different pressure levels, i.e. 5, 7.5 and 10 psi, adjusted with a pressure regulator. Each data measurement was done for 5 seconds at 1 KHz. The sensor’s reading was calibrated before each measurement.

2) RESULT AND DISCUSSION

The result of vibration acceleration measurement for different frequencies is provided in Fig. 8. It can be observed that the acceleration of the vibration signal drops with the increase in the signal frequency. This pattern persists across all set pressure levels, both in normal and lateral directions. Specifically, the acceleration values range between 3.15 g

(20 Hz at 10 psi) and 0.15 g (250 Hz at 5 psi) in the normal direction. On the other hand, the lateral measurements change from 2.05 g (20 Hz at 10 psi) to 0.19 g (250 Hz at 7.5 psi). Importantly, the vibration acceleration produced at varying frequencies surpasses the threshold for human perception of vibrations, with even the smallest measured acceleration, that is, 0.15 g or 1.47 m/s<sup>2</sup> at 250 Hz and 5 psi, remaining above the sensitivity limit [34], [35], [36].

In order to verify if the rendered vibration signal truly rendered the targeted frequency, a sample vibration data is recorded of a signal rendered with 100 Hz frequency at 7.5 psi. Fig. 9 (a) shows the recorded signal in the time domain while Fig. 9 (b) shows the corresponding frequency spectrum. The system rendered a 100 Hz frequency signal with a minor error of 1% as the recorded signal showed a peak at 99 Hz.

Vibrations below 20 Hz at 10 psi were not recorded in the normal direction due to concerns about damaging the silicon air cell due to prolonged exposure to high pressures. However, lesser pressures of 5 psi and 7.5 psi did not pose the same harm and were used for low-frequency vibrations. This adverse effect was not observed in the lateral direction, as the cylindrical housing combined with the piston-shaped holder adeptly absorbed and transmitted all linear motion to the NAU. Furthermore, during the experimental phase, it was discerned that lateral vibrations capped at 150 Hz ( at 5 psi) as a rapid change in pressure failed to induce noticeable vibrations in the apparatus.

B. PRESSURE FEEDBACK MEASUREMENT

NAU and LAUs are responsible for normal force (pressure) and lateral force feedback. In the case of normal force rendering, the valve control mechanism is shown in Fig. 6(b). For lateral force rendering, the valve opening mechanism is

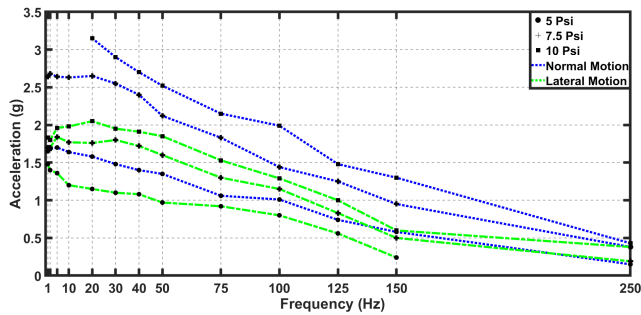


FIGURE 8. Valve control mechanism to produce different forms of actuation.

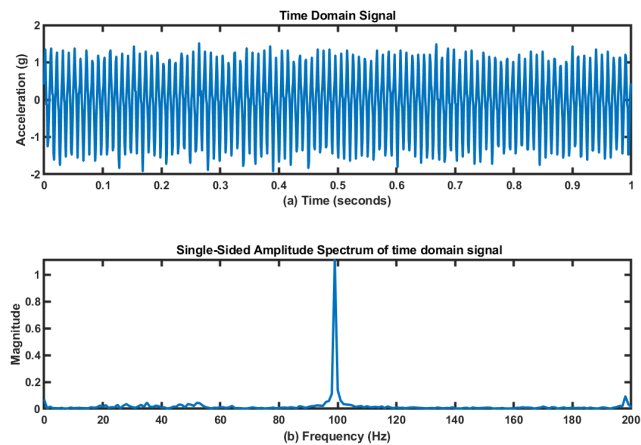


FIGURE 9. Time domain and respective frequency spectrum of the 100 Hz signal rendered at 7.5 psi.

similar as explained in Fig 6(b), however, the direction of motion in lateral space is controlled by the valve opening patterns in Fig. 6(d).

### 1) MEASUREMENT PROCEDURE

To measure the force output of the device, a force sensor (Wenzhou SF20) is used. The device was placed in two different setups to measure the normal force and lateral force. For normal force, the sensor is placed right above the actuation point as illustrated in Fig. 10 (a). The data was recorded for 3 pressure levels i.e. 5, 7.5, and 10 Psi. For each pressure level, the air pressure inside the air cell was changed by opening the positive valve from 0 to 250ms with a step size of 10 ms. At each step size, a static pressure was generated in the air cell, and the data was recorded. This measurement procedure was repeated 3 times and the data points were averaged for each step size.

For lateral force measurement, a 3D-printed module was attached with NAU (illustrated in Fig. 10 (b)), so that the force from the lateral APs could be transferred to the force sensor. During measurement, the same pressure levels were used. The goal was to measure the maximum force in 2 directions i.e. lateral, and diagonal, based on the pressure levels. Therefore, force data at each pressure level were recorded in each direction. The pressure inside the air cell was

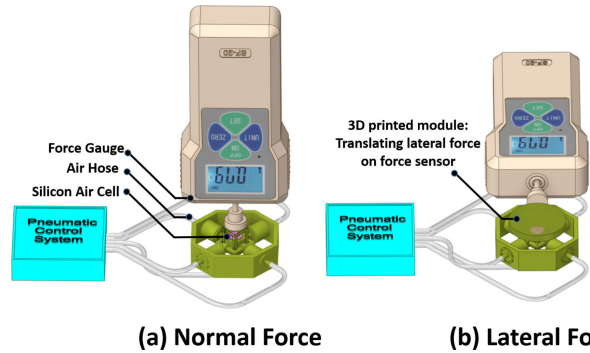


FIGURE 10. Force measurement setup.

maintained for recording the data. The same pressure levels and step size are used for normal force.

### 2) RESULT AND DISCUSSION

Figure 11 depicts the relationship between the force magnitude and the duration of valve opening. As anticipated, there's a direct correlation between the force output and the duration for which the valve remains open. For the initial 100 ms, there's a noticeable change in force output across all three directions. This rapid force increase tapers off by 150 ms and saturates, maintaining a near-constant force until 250 ms. The peak force observed is 8.3N (with a valve opening of 250 ms at 10 psi) in the normal direction. Yet, there's a risk of damaging the silicon air cell if the solenoid valve stays open beyond 250 ms at an input pressure of 10 psi. Hence, the safest maximum force that can be achieved is approximately 8 N in the normal direction. Nevertheless, the output force of 8 N is still well within the range suitable for a variety of applications involving haptic feedback [37].

It must be noted that the response time of the solenoid valve is 2 ms in the pneumatic control system. The force control of the system is dependent upon the input pressure and the solenoid valve opening duration. Considering the solenoid valve requires at least 2 ms to open, the finest resolution of control you can achieve is bounded by this minimum actuation time. This is except for scenarios involving lateral force at 5 psi and 7.5 psi, which necessitated valve openings of 5 ms and 3 ms, respectively, to achieve a consistent force variation. Within the transient time phase, the force resolution varies from 0.02 N to 0.11 N depending on the input pressure and direction of motion. Complete details of force resolution are provided in the Table 1.

The overall measurement experiment shows that the actuator's static output can be controlled with time delay input to the solenoid valve opening. Beyond static output, these time delays can also be controlled dynamically to render the dynamically changing output of the actuator. The dynamic output can be controlled by an algorithm where the time delay of the rendered signals can be stored/logged to measure how much force has been registered into the device already, and how much more time delay is needed to reach the targeted output force.

**TABLE 1.** Force resolution w.r.t. different direction of actuation and minimum valve opening time during transient time phase.

Direction	Pressure (Psi)	Force Resolution (N)	Valve opening duration (ms)	Transient time (ms)
Lateral	5	0.02	5	90
	7.5	0.02	3	90
	10	0.03	2	90
Diagonal	5	0.02	2	70
	7.5	0.04	2	70
	10	0.06	2	70
Normal	5	0.02	2	90
	7.5	0.07	2	60
	10	0.11	2	60

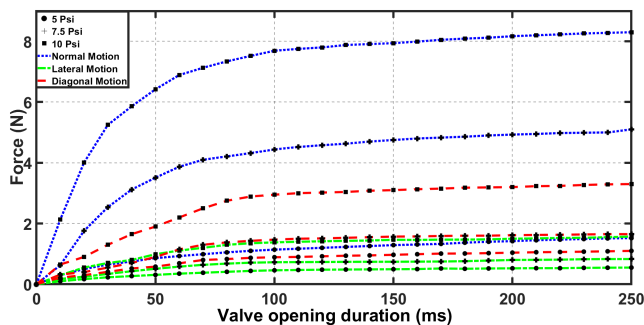


**FIGURE 11.** Force measurement against positive valve opening duration.

**TABLE 2.** Displacement measurement based on controlling a pair of valves. Data measured at a set pressure of 10 psi.

FAP valve opening (ms)	12	12	12	12	9	6	6	9	6	3	0
BAP valve opening (ms)	0	3	6	9	6	6	9	12	12	12	12
Distance (mm)	6	4.48	2.26	0.75	1.49	0	1.47	0.76	2.24	4.51	6
Standard deviation (mm)	0	0.18	0.12	0.07	0.1	0	0.1	0.08	0.12	0.17	0
	Backward Motion			Center			Forward Motion				

**C. LATERAL MOTION**

One of the key features of the device is its ability to guide the end effector laterally. Fig. 6 (e) depicts the mechanism of valve regulation for attaining this sideways movement. Through this mechanism, users can direct the end effector toward a particular path by managing the input pressure and the duration of a solenoid valve’s opening. Further description of the position control process is discussed in the subsequent sections.

**1) MEASUREMENT PROCEDURE**

In the process of lateral motion control, one solenoid valve introduces air, propelling the end effector to generate a linear shift. Simultaneously, its opposite solenoid valve delivers air to exert a counteracting force, thereby constraining the extent of the shift. The degree of displacement can be managed by adjusting the time delay of each solenoid valve’s activation. To monitor the positional variation in the end effector, the activation delay for the solenoid valves was sequentially adjusted between 0 ms and 12 ms in increments of 3 ms. Displacement measurements were conducted using a dial calliper. The resolution of the slide calliper was 0.01 mm.

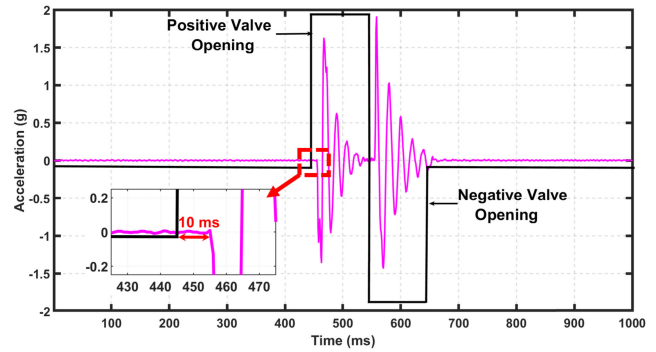


**FIGURE 12.** System’s response time measurement result.

The data for each positional variation was recorded five times and the rounded mean of the displacement was calculated.

The pressure input was maintained at 10 psi during the measurement.

**2) RESULTS AND DISCUSSION**

Table 2 displays the results of the changes in position that took place upon manipulating a pair of solenoid valves situated in opposing directions, utilizing various combinations of time delays. Notably, the device achieved a displacement spanning 12 mm, implying a peak shift of 6 mm on either side from the central point with a standard deviation in the range of 0.18 mm. Straightforwardly, diagonal movement can be achieved by regulating all four APs, each with distinct time delays.

It’s worth admitting that this assessment was specifically concentrated on the effect of valve control for lateral motion or force, not on the precise control of the end-effector’s position. Open-loop travel distance control may not work under different lateral resistances caused by contact between the end-effector and the user’s skin, which even changes under different normal direction pressures.

**D. SYSTEM’S RESPONSE TIME**

The actuation delay is a critical factor in pneumatic systems, directly affecting the quality of perceived haptic feedback. This section examines the response time of the proposed pneumatic system.

**1) MEASUREMENT PROCEDURE**

The system’s response time was determined by sending a step signal to the actuator and monitoring the acceleration response using the setup illustrated in Fig 7. The procedure involved activating the positive valve for 100 ms to generate a distinct impact, followed by a 100 ms activation of the negative valve to reset the actuator. Acceleration data was captured at a frequency of 1 kHz, and the delay between the initiation of the step signal and the onset of acceleration was calculated.

**2) RESULTS AND DISCUSSION**

The response time, as shown in Fig. 12, indicated an approximate delay of 10 ms from the step signal to the start

**TABLE 3. Performance comparison of the proposed work with the available state-of-the-art related works. (N/A: Not Available, NR: Not Reported).**

Study	Actuation Method	Form Factor		Simultaneous Actuations	Max Output				
		Size	Weight		Normal Force	Shear Force	Normal Vibration	Lateral Vibration	Frequency Range
Kanjanapas [21] (2019)	Pneumatic	48.8 x 48.8 (mm)	150 g	No	1 N	N/A	N/A	N/A	N/A
Yoshina [7] (2019)	Pneumatic and DC motor	113 mm diameter 30mm height	82 g	Yes	1.3 N	0.47 N	NR	NR	NR
Zhakypov [27] (2022)	Pneumatic	40 x 20 (mm)	13.7 g	No	7N	1.3N	NR	NR	1 - 64 Hz
Talhan [6] (2019)	Pneumatic	100 mm length	4.5 g	No	6.3 N	N/A	2.2 g	N/A	1-250 Hz
Pezent [20] (2022)	DC motor	50 x 30 x 15 (mm)	120 g	No	15N	1.2 N	NR	N/A	0-15 Hz
Thai [38] (2020)	DC motor	12 mm diameter 2mm height	4.3 g	No	N/A	1.8 N	N/A	N/A	N/A
<b>Proposed</b>	Pneumatic	55 x 55x 20 (mm)	25 g	Yes	8.3 N	3.3 N	3.15 g	2.05 g	1 - 250 Hz

of acceleration. This response time is influenced by several components, including the reaction time of the electronic valves, the pressure of the air source, and the hose's physical attributes [6], [39], [40].

The rapid response time of the proposed actuator can be attributed to three key factors. First, the solenoid valve's minimal latency, notably 2 milliseconds, ensures swift control over the valve states. Second, the CO<sub>2</sub> tank's high-pressure gas facilitates rapid air movement through the hose, allowing the system to react promptly to actuation commands. Finally, the thin soft silicone air cell is designed for rapid actuation as soon as it is filled with air.

It is to be noted that a delay of 10 ms is imperceptible. For visual-tactile stimulation, the perception of temporal delay depends upon the sequence of stimulus presentation, whether visual or tactile stimuli are presented first. Research has shown that the perception threshold of temporal delay during a visual-tactile rendering event ranges from 27 ms to 71 ms [41], [42]. Hence, a 10 ms delay can be considered perceptually negligible in the presentation of visual-tactile stimuli.

### E. PERFORMANCE METRICS COMPARISON

The device's performance was assessed by evaluating its principal attributes and comparing them with those reported in similar research. The comparison focused on several key aspects: normal and shear forces, and vibration acceleration in both normal and lateral orientations. The presence of simultaneous actuation and the range of frequency bandwidth were also considered. Features that are absent in the compared studies are indicated as 'N/A' for not available. Meanwhile, features that are acknowledged by the reference study but lack any empirical characterization are marked as 'NR', which stands for not reported.

Table 3 presents a comparison of various tactile devices based on several performance metrics and characteristics. The proposed pneumatic actuator stands out with its capacity for simultaneous actuation and a wide frequency range of 1-250 Hz, matching the upper limit of Talhan et. al. [6] pneumatic actuator. It also shows a significant improvement

in maximum output force with 8.3 N normal force and 3.3 N shear force, which is higher than any other pneumatic actuator listed. It's worth mentioning that the proposed device is comparatively heavier at 25 g than some actuators, however, all the lightweight actuators were not able to achieve higher performance in comparison to the proposed actuator.

The ability to provide simultaneous actuation is a key feature that may enable more complex haptic feedback, and this feature is only present in two devices listed, including the proposed actuator. In terms of actuation method, pneumatic systems seem to dominate, except [20] and [38], which use DC motors, indicating a variation in the design approach to achieve tactile feedback. The proposed device provides a robust range of capabilities, suggesting that it might be better suited for applications requiring a more dynamic haptic response.

## VII. USER PERCEPTION EXPERIMENT

In section VI, the device's performance is estimated with a series of measurement experiments. The device is found to be able to render strong lateral cues and vibrotactile feedback e. However, to confirm the effectiveness of this quantitative observation, a user perception experiment is designed. The main goal of this experiment is to identify if the users can easily identify the difference between lateral cues and vibration signals rendered with different frequencies.

### A. PARTICIPANTS

A total of 15 participants (Thirteen males and two females) took part in the perception experiment. Their age ranged from 25 to 34 with an average of 29.06. All the participants were healthy and fit to take part in the experiment. An informed consent was also obtained for taking part in the experiment from each participant.

### B. PROCEDURE

The perception experiment was meticulously designed to assess the efficacy of lateral and vibration feedback mechanisms. Initially, participants were introduced to lateral cues in four distinct directions: forward, backward, right, and left,

### Contact area Points



**FIGURE 13.** A participant taking part in the experiment. The contact area is also highlighted creating no contact force between the body site and the end-effector when attached to the body.

applied to the forearm. The device's attachment was precisely oriented to intuitively correspond with the user's body: forward towards the hand, backward towards the elbow, right towards the thumb, and left to the opposite side. This setup aimed to provide clear and distinguishable directional cues through the movement of the end-effector along specified paths.

In addition to lateral cues, the experiment evaluated vibration feedback through the presentation of three different signal frequencies: 40 Hz, 80 Hz, and 120 Hz. This component was designed to test participants' ability to discern variations in frequency, further contributing to our understanding of sensory perception under varying vibratory conditions.

The experimental setup was calibrated with specific attention to the input pressures and contact forces to ensure consistent delivery of stimuli while maintaining participant comfort. Lateral cues were administered with an input pressure of 10 psi and a normal contact force of 1 N, whereas vibratory feedback was provided at a slightly reduced pressure of 7.5 psi. To prevent direct contact between the device's end-effector and the participant's skin, a contact area is integrated into the design, as shown in Fig 13. The depth of the contact area is higher than the end-effector, therefore, in rest condition the end-effector hovers just above the skin and not in contact.

Before the commencement of the experiment, participants underwent a comprehensive briefing session, accompanied by a practice session aimed at acquainting them with the haptic cues. This preparatory phase was essential for familiarizing participants with the experimental environment and ensuring accurate response collection. During the experiment, the lateral actuation point was pressurized by opening the valve for 150 ms and the cue was presented for 2 seconds, after which participants were asked to identify

the cue's direction. To eliminate potential biases and ensure the reliability of responses, the presentation order of the cues was randomized, and participants were given the option to request a repetition of any cue. Following the lateral cues, participants were subjected to vibration stimuli, where they were asked to match a test stimulus with one of three subsequent stimuli in a similar randomized fashion. This methodology, encompassing a total of 105 trials across all participants, was employed to gather a dataset for analysis.

Figure 13 shows the experimental environment. The participants wore headphones with white noise to remove environmental noise. The forearm attached with actuation was rested on a table, and a visual barrier was introduced between the participant's vision and arm so that the participant could focus only on the instructions and the stimulus presented.

### C. RESULTS AND DISCUSSION

The results, shown in Fig 14, clearly show that all the participants showed 100% accuracy for vibration feedback. This explains why the participants were able to feel the difference between the presented stimuli. On the other hand, for lateral cues, the overall perception accuracy for identifying lateral cues was 88.33%. The highest and lowest individual accuracy from the participants were found 100% and 50% respectively. While the majority of the participants were able to recognize the lateral cue accurately.

In the experiment, higher accuracy was achieved possibly due to the lateral housing as it guides the inflation of air cell and converts all the pressure into linear translation. Additionally, the end-effector stays in stable contact with the skin when the lateral cue is rendered. In haptic literature, it is found that the perception of tangential force increases as the magnitude of applied normal force as an analysis was conducted on the perceived magnitude of shear force between 0.1 N to 0.7 N [43]. Kanjanapas et al. reported that a shear force of 0.23N applied on the user's forearm with just 1 mm displacement allows users to perceive the direction of lateral stimulus [21]. During the perception experiment, the lateral cues were rendered at around 1.7 N shear force, which is quite higher than the human perception range and helped to achieve accurate user response.

### VIII. USER EXPERIENCE STUDY

To evaluate the effectiveness of the developed haptic device and its integration in real-world scenarios, we conducted a study focusing on the subjective experiences of users. This study involved participants who interacted with the device in a gaming environment.

#### A. PARTICIPANTS

The study comprised 15 individuals (twelve males and three females), with an average age of 28.75 years (ranging from 26 to 33 years). None of the participants reported any physical impairments that could affect their ability to participate in the experiment. Before participating, all

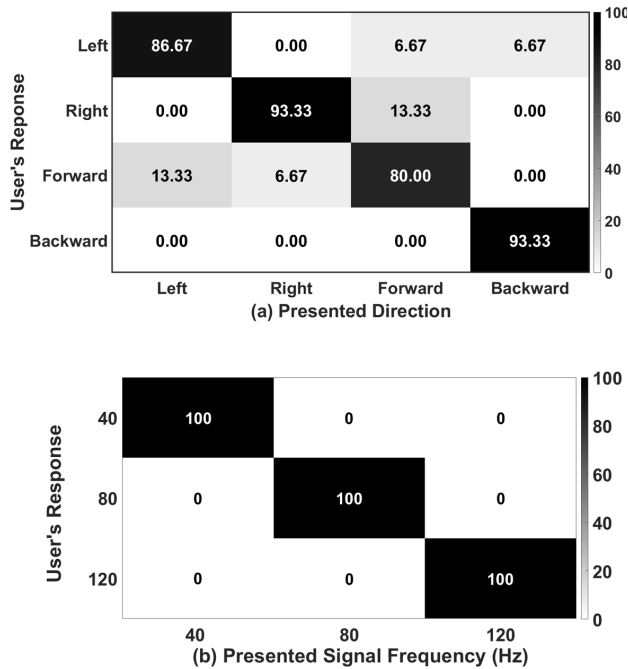


FIGURE 14. Confusion matrix showing results for (a) Direction Classification and (b) vibration classification.



FIGURE 15. Subjective experiment scenario: A participant playing a game while the proposed device is attached to the wrist.

individuals were provided with a detailed explanation of the study’s nature and objectives. Informed consent was obtained from each participant, ensuring they understood the procedures and their rights.

**B. PROCEDURE**

The study utilized a first-person shooter (FPS) game scenario created in Unity3D to assess the device’s performance and compare it with conventional gameplay experiences. The participants were asked to use a mouse to control the gun and shoot the targets present in the scene. The device was attached to each participant’s wrist using a Velcro strap. To ensure an immersive experience and minimize external distractions, participants were provided with headphones to block outside noise. The evaluation environment is shown in Fig. 15.

Three different gameplay modes were presented: 1) Audio-Visual (AV) feedback, 2) Audio-Visual with Haptic (AVH) feedback, and 3) Audio-Visual with Multi-modal Haptic (AVMH) feedback. In the AV mode, participants experienced the game with standard audio-visual feedback. The AVH mode added single-impact feedback from NAU upon firing a gun, simulating the gunshot impact. The AVMH mode provided combined haptic feedback; impact from the NAU and short burst lateral motion effect from the two LAUs mimicking the gun’s recoil effect. The order of these modes was randomized for each participant to reduce any potential bias.

**C. FEEDBACK QUESTIONNAIRE**

The study aimed to evaluate various aspects such as the quality of feedback, user experience, and device response time. The questionnaire was designed based on the guidelines from standardized tools for assessing game and haptic experiences [44], [45]. It included six questions, three of which focused on feedback quality, addressing immersion, sensory and imaginative (S & I) feedback, and expressivity. Two questions explored user engagement and experience enhancement during gameplay. The final question assessed the flow of the game in different modes to gauge the system’s response time. Participants rated their responses on a Likert scale ranging from 1 (strongly disagree) to 7 (strongly agree). Additionally, they were given the opportunity to provide general feedback about their experience. The factors with descriptions presented to the participants in the feedback questionnaire are shown in Table 4. The complete questionnaire can be found in Appendix.

**D. RESULTS AND DISCUSSION**

Participant feedback was aggregated and assessed by computing the mean of the Likert scale scores for all factors within each experimental condition. The outcomes of this assessment are shown in Fig. 16. In this figure, the bar graph illustrates the average scores participants assigned on the Likert Scale, while the accompanying error bars represent the standard deviation of these scores. It is evident from the graph that the device’s AVMH mode (mode 3) outperformed other modes across most of the individual factors. To further examine the data, a one-way analysis of variance (ANOVA) was employed to determine both the mean values and the statistical disparities across the different conditions. This was complemented by a post hoc pairwise comparison test applying the Tukey-Kramer method to analyze specific differences.

The analysis showed that the modes incorporating haptic feedback (AVH and AVMH) were statistically significantly ( $p < 0.05$ ) better than conventional gameplay systems in all individual factors, except *Flow*. It should be noted that the lack of statistical difference ( $p > 0.05$ ) for the factor *Flow* confirmed that the participants found the proposed device’s actuation was well connected with the user’s actions

**TABLE 4.** The psychophysical experiment’s factors and corresponding descriptions were presented to participants during the evaluation.

Sr.	Factors	Description
1.	<b>Immersion:</b>	The gameplay helped me to focus on the task
2.	<b>Sensory and Imaginative Feedback:</b>	The feedback received helped in visualizing and experiencing the game’s environment more intensely.
3.	<b>Expressivity:</b>	The gameplay helped me distinguish what was going on.
4.	<b>Experience:</b>	The feedback provided by the game improved my overall experience
5.	<b>Engagement:</b>	I felt connected to the game’s actions
6.	<b>Flow:</b>	I experienced a smooth progression of game activities.
7.	<b>General Comments:</b>	

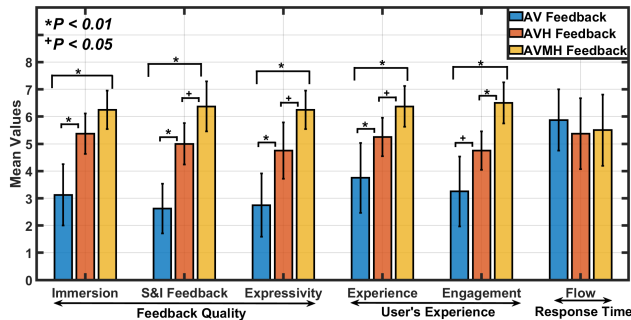


**FIGURE 16.** Psychophysical evaluation result.

while playing the game with AV feedback. For all other factors, the data indicated a clear preference among users for the multimodal haptic feedback, as it appeared to enrich their gameplay experience. In addition to quantitative data, qualitative feedback was also gathered. One participant commented, “This particular feedback (referred to as mode 3) felt better and I enjoyed it while playing the game”. Another participant commented, “I prefer playing games with special effects (mode 3) generated by the device than the other modes”

**IX. GENERAL DISCUSSION**

The primary objective of the work was to render different types of haptic feedback through a single end-effector. As explained in Section VI, the actuator’s characterization showed its ability to deliver diverse tactile sensations, a capability further affirmed by the user perception experiment. This experiment, designed to determine users’ ability to differentiate between lateral cues and vibration frequencies, validated the actuator’s effectiveness in providing distinct tactile feedback. The actuator’s design enables simultaneous actuation from all the APs, which are controlled independently. This feature is important in rendering multimodal tactile feedback effectively. The results from the subjective evaluations further support the success of the actuator in achieving its intended purpose. Participants in the study consistently reported that the AVMH feedback significantly enhanced their interactive experiences. We particularly note that the higher scores in the factor *expressivity* confirm that the multiple feedback added a significant level of detail to their in-game actions. These positive responses from the participants show the potential of the actuator.

The actuator’s design utilizes 3D printing with ABS material and flexible soft silicon. This simple design ensures easy integration. However, we noted that it’s important to

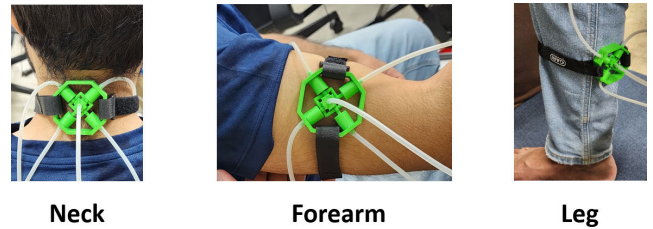


**FIGURE 17.** Example attachment scenarios for different body sites.

Name and Age:

Please rate each statement based on your experience with the game under the condition. Provide your rating on a scale from 1 (Strongly Disagree) to 7(Strongly Agree).

**Immersion:**

- The Game play helped me to focused on the task

Mode 1:	Strongly disagree	1	2	3	4	5	6	7	Strongly Agree
Mode 2:	Strongly disagree	1	2	3	4	5	6	7	Strongly Agree
Mode 3:	Strongly disagree	1	2	3	4	5	6	7	Strongly Agree

**Sensory and Imaginative Feedback:**

- The feedback received helped in visualizing and experiencing the game’s environment more intensely.

Mode 1:	Strongly disagree	1	2	3	4	5	6	7	Strongly Agree
Mode 2:	Strongly disagree	1	2	3	4	5	6	7	Strongly Agree
Mode 3:	Strongly disagree	1	2	3	4	5	6	7	Strongly Agree

**Expressivity:**

- The game play helped me distinguish what was going on.

Mode 1:	Strongly disagree	1	2	3	4	5	6	7	Strongly Agree
Mode 2:	Strongly disagree	1	2	3	4	5	6	7	Strongly Agree
Mode 3:	Strongly disagree	1	2	3	4	5	6	7	Strongly Agree

**Experience:**

- The feedback provided by the game (if any) improved my overall experience

Mode 1:	Strongly disagree	1	2	3	4	5	6	7	Strongly Agree
Mode 2:	Strongly disagree	1	2	3	4	5	6	7	Strongly Agree
Mode 3:	Strongly disagree	1	2	3	4	5	6	7	Strongly Agree

**Engagement:**

- I felt connected to the game actions

Mode 1:	Strongly disagree	1	2	3	4	5	6	7	Strongly Agree
Mode 2:	Strongly disagree	1	2	3	4	5	6	7	Strongly Agree
Mode 3:	Strongly disagree	1	2	3	4	5	6	7	Strongly Agree

**Flow:**

- I experienced a smooth progression of game activities.

Mode 1:	Strongly disagree	1	2	3	4	5	6	7	Strongly Agree
Mode 2:	Strongly disagree	1	2	3	4	5	6	7	Strongly Agree
Mode 3:	Strongly disagree	1	2	3	4	5	6	7	Strongly Agree

**General Comments:**

**FIGURE 18.** Feedback questionnaire.

precisely integrate the silicon air cells with the 3D-printed parts to prevent air leakage, which can impair the actuator’s performance. Additionally, high input pressure was found to damage the silicon air cells. Therefore, it’s advisable to monitor the input pressure carefully, ensuring it remains below 10 psi to avoid such issues.

The user study assessed the performance of the actuator when placed on the wrist. The design of the actuator

incorporates a velcro strap, which allows for its application to various parts of the body, a concept demonstrated in Figure 17. If the actuator is positioned in different locations such as the leg or neck, the resultant sensory experience may vary due to the unique vibratory thresholds and considerations of comfort at each site. Therefore, it is crucial to tailor the actuator's settings to each particular location to achieve the intended sensory feedback. However, except for the human hand, which displays an increased sensitivity compared to other regions, the tactile sensitivity across various body sites tends to show a comparable level of perception [46], [47], [48]. This uniformity in sensitivity suggests that the standardization of input parameters is feasible, simplifying the process of calibrating the actuator for different body parts.

The actuator has various applications; in construction safety training, trainees can attach it to their wrists to feel forces and vibrations akin to using tools, aiding in correct equipment usage and reducing accidents. In gaming, when worn on the legs, it simulates impacts and tremors, enhancing immersion. Virtual tours, help users sense environmental elements, like moving objects. These uses demonstrate the device's adaptability across different body sites and its ability to improve user experience.

#### A. FUTURE WORK

The device's capability to render multiple tactile stimulations can yield certain perceptual effects such as masking, summation etc [49]. This necessitates further exploration into how multiple tactile stimulations affect user perception. To address this, future plans include conducting psychophysical experiments with subjects. The goal of these experiments is to develop guidelines for creating application scenarios that effectively utilize multiple tactile sensations with the system.

#### X. CONCLUSION

In summary, this research presents a novel multimodal pneumatic haptic actuator, adeptly designed for a wide range of wearable haptic feedback. The integration of a 3D-printed structure with soft silicon air cells, and a pneumatic system, allows the device to provide diverse tactile feedback forms, including vibration, pressure, and lateral forces, efficiently through a single end-effector. The actuator has been characterized, demonstrating its capability to produce a range of tactile sensations with considerable force and frequency. Moreover, the user experience study highlights the device's practical effectiveness and the added value it brings to immersive environments. Weighing the benefits and versatility of the actuator, it stands out as a significant contribution to the field of wearable haptic technology, offering promising applications in areas such as virtual reality, gaming, and interactive training simulations.

## APPENDIX FEEDBACK QUESTIONNAIRE FOR USER EXPERIENCE STUDY

Figure 18 shows the actual questionnaire presented to the user during the study.

#### REFERENCES

- [1] N. Magnenat-Thalmann and U. Bonanni, "Haptics in virtual reality and multimedia," *IEEE MultimediaMag.*, vol. 13, no. 3, pp. 6–11, Jul. 2006.
- [2] F. Danieau, A. Lecuyer, P. Guillotel, J. Fleureau, N. Mollet, and M. Christie, "Enhancing audiovisual experience with haptic feedback: A survey on HAV," *IEEE Trans. Haptics*, vol. 6, no. 2, pp. 193–205, Apr. 2013.
- [3] Y. Huang, K. Yao, J. Li, D. Li, H. Jia, Y. Liu, C. K. Yiu, W. Park, and X. Yu, "Recent advances in multi-mode haptic feedback technologies towards wearable interfaces," *Mater. Today Phys.*, vol. 22, Jan. 2022, Art. no. 100602.
- [4] M.-W. Ueberle, "Design, control, and evaluation of a family of kinesthetic haptic interfaces," Ph.D. dissertation, Elektrotechnik und Informationstechnik, Technische Universität München, München, Germany, 2006.
- [5] R. E. S. Cruz, M. C. Coffey, A. Y. Sawaya, and R. P. Khurshid, "Modular haptic feedback for rapid prototyping of tactile displays," in *Proc. IEEE World Haptics Conf. (WHC)*, Jul. 2021, pp. 703–708.
- [6] A. Talhan, H. Kim, and S. Jeon, "Tactile ring: Multi-mode finger-worn soft actuator for rich haptic feedback," *IEEE Access*, vol. 8, pp. 957–966, 2020.
- [7] K. T. Yoshida, C. M. Nunez, S. R. Williams, A. M. Okamura, and M. Luo, "3-DoF wearable, pneumatic haptic device to deliver normal, shear, vibration, and torsion feedback," in *Proc. IEEE World Haptics Conf. (WHC)*, Jul. 2019, pp. 97–102.
- [8] J. Qi, F. Gao, G. Sun, J. C. Yeo, and C. T. Lim, "HaptGlove—Untethered pneumatic glove for multimode haptic feedback in reality—virtuality continuum," *Adv. Sci.*, vol. 10, no. 25, Sep. 2023, Art. no. 2301044.
- [9] J. Chen, E. H. T. Teo, and K. Yao, "Electromechanical actuators for haptic feedback with fingertip contact," *Actuators*, vol. 12, no. 3, p. 104, Feb. 2023.
- [10] J.-H. Koo, J. M. Schuster, T. Tantiartyanontha, Y.-M. Kim, and T.-H. Yang, "Enhanced haptic sensations using a novel electrostatic vibration actuator with frequency beating phenomenon," *IEEE Robot. Autom. Lett.*, vol. 5, no. 2, pp. 1827–1834, Apr. 2020.
- [11] G. G. Poyraz and Ö. Tamer, "Different haptic senses with multiple vibration motors," in *Proc. 11th Int. Conf. Electr. Electron. Eng. (ELECO)*, Nov. 2019, pp. 870–874.
- [12] S. Doerger and C. Harnett, "Force-amplified soft electromagnetic actuators," *Actuators*, vol. 7, no. 4, p. 76, Oct. 2018.
- [13] S. Choi and K. J. Kuchenbecker, "Vibrotactile display: Perception, technology, and applications," *Proc. IEEE*, vol. 101, no. 9, pp. 2093–2104, Sep. 2013.
- [14] J. Rantala, P. Majaranta, J. Kangas, P. Isokoski, D. Akkil, O. Špakov, and R. Raisamo, "Gaze interaction with vibrotactile feedback: Review and design guidelines," *Human-Comput. Interact.*, vol. 35, no. 1, pp. 1–39, Jan. 2020.
- [15] S. Kim, B. Son, Y. Lee, H. Choi, W. Lee, and J. Park, "A two-DOF impact actuator for haptic interaction," in *Haptic Interaction: Perception, Devices Algorithms*, vol. 3. Singapore: Springer, 2019, pp. 173–177.
- [16] M. Matysek, P. Lotz, and H. F. Schlaak, "Tactile display with dielectric multilayer elastomer actuators," in *Electroactive Polymer Actuators and Devices (EAPAD)*, vol. 7287. Bellingham, WA, USA: SPIE, 2009, pp. 425–433.
- [17] I. Mo Koo, K. Jung, J. Choon Koo, J.-D. Nam, Y. Kwan Lee, and H. R. Choi, "Development of soft-actuator-based wearable tactile display," *IEEE Trans. Robot.*, vol. 24, no. 3, pp. 549–558, Jun. 2008.
- [18] J.-B. Biernacki, P.-W. Kao, S. S. Tiruvaipati, and P. M. Scholl, "Feel the pressure: A haptic-feedback device for wearable musical instrument interaction," in *Adjunct Proc. ACM Int. Joint Conf. Pervasive Ubiquitous Comput. Proc. ACM Int. Symp. Wearable Comput.*, Sep. 2019, pp. 254–256.
- [19] E. Pezent, A. Israr, M. Samad, S. Robinson, P. Agarwal, H. Benko, and N. Colonnese, "Tasbi: Multisensory squeeze and vibrotactile wrist haptics for augmented and virtual reality," in *Proc. IEEE World Haptics Conf. (WHC)*, Jul. 2019, pp. 1–6.

- [20] E. Pezent, P. Agarwal, J. Hartcher-O'Brien, N. Colonnese, and M. K. O'Malley, "Design, control, and psychophysics of tasbi: A force-controlled multimodal haptic bracelet," *IEEE Trans. Robot.*, vol. 38, no. 5, pp. 2962–2978, Oct. 2022.
- [21] S. Kanjanapas, C. M. Nunez, S. R. Williams, A. M. Okamura, and M. Luo, "Design and analysis of pneumatic 2-DoF soft haptic devices for shear display," *IEEE Robot. Autom. Lett.*, vol. 4, no. 2, pp. 1365–1371, Apr. 2019.
- [22] F. Chinello, M. Aurilio, C. Pacchierotti, and D. Prattichizzo, "The hapband: A cutaneous device for remote tactile interaction," in *Proc. 9th Int. Conf. Haptics, Neurosci., Devices, Model., Appl. (EuroHaptics)*, Versailles, France. Berlin, Germany: Springer, 2014, pp. 284–291.
- [23] M. Aggravi, F. Pausé, P. R. Giordano, and C. Pacchierotti, "Design and evaluation of a wearable haptic device for skin stretch, pressure, and vibrotactile stimuli," *IEEE Robot. Autom. Lett.*, vol. 3, no. 3, pp. 2166–2173, Jul. 2018.
- [24] H.-Y. Chang, W.-J. Tseng, C.-E. Tsai, H.-Y. Chen, R. L. Peiris, and L. Chan, "FacePush: Introducing normal force on face with head-mounted displays," in *Proc. 31st Annu. ACM Symp. User Interface Softw. Technol.*, 2018, pp. 927–935.
- [25] S. Günther, D. Schön, F. Müller, M. Mühlhäuser, and M. Schmitz, "PneumoVolley: Pressure-based haptic feedback on the head through pneumatic actuation," in *Proc. Extended Abstr. CHI Conf. Human Factors Comput. Syst.*, Apr. 2020, pp. 1–10.
- [26] A. Talhan, S. Kumar, H. Kim, W. Hassan, and S. Jeon, "Multi-mode soft haptic thimble for haptic augmented reality based application of texture overlaying," *Displays*, vol. 74, Sep. 2022, Art. no. 102272.
- [27] Z. Zhakypov and A. M. Okamura, "FingerPrint: A 3-D printed soft monolithic 4-degree-of-freedom fingertip haptic device with embedded actuation," in *Proc. IEEE 5th Int. Conf. Soft Robot. (RoboSoft)*, Apr. 2022, pp. 938–944.
- [28] M. Zhu, S. Biswas, S. I. Dinulescu, N. Kastor, E. W. Hawkes, and Y. Visell, "Soft, wearable robotics and haptics: Technologies, trends, and emerging applications," *Proc. IEEE*, vol. 110, no. 2, pp. 246–272, Feb. 2022.
- [29] S. Kim, H. Kim, B. Lee, T.-J. Nam, and W. Lee, "Inflatable mouse: Volume-adjustable mouse with air-pressure-sensitive input and haptic feedback," in *Proc. SIGCHI Conf. Human Factors Comput. Syst.*, Apr. 2008, pp. 211–224.
- [30] C. Harrison and S. E. Hudson, "Providing dynamically changeable physical buttons on a visual display," in *Proc. SIGCHI Conf. Human Factors Comput. Syst.*, Apr. 2009, pp. 299–308.
- [31] A. Stevenson, C. Perez, and R. Vertegaal, "An inflatable hemispherical multi-touch display," in *Proc. 5th Int. Conf. Tangible, Embedded, Embodied Interact.*, Jan. 2010, pp. 289–292.
- [32] B. Li, B. Greenspan, T. Mascitelli, M. Raccuglia, K. Denner, R. Duda, and M. A. Lobo, "Design of the playskin air: A user-controlled, soft pneumatic exoskeleton," in *Frontiers in Biomedical Devices*, vol. 41037. New York, NY, USA: American Society of Mechanical Engineers, 2019, Art. no. V001T03A004.
- [33] Chris. (2015). *Controlling A Solenoid Valve With Arduino*. [Online]. Available: <https://bc-robotics.com/tutorials/controlling-a-solenoid-valve-with-arduino/>
- [34] A. Picu, "Study about evaluation of human exposure to hand-transmitted vibration," *J. Sci. Arts*, vol. 2, no. 13, pp. 355–360, 2010.
- [35] T. Hempstock and D. O'connor, "Evaluation of human exposure to hand-transmitted vibration," *Appl. Acoust.*, vol. 8, no. 2, pp. 87–99, 1975.
- [36] M. Morioka and M. J. Griffin, "Perception thresholds for lateral vibration at the hand, seat, and foot," *Hand*, vol. 1, no. 10, p. 100, 2006.
- [37] R. Balasubramanian and V. J. Santos, *The Human Hand as an Inspiration for Robot Hand Development*, vol. 95. Switzerland: Springer, 2014.
- [38] M. T. Thai, T. T. Hoang, P. T. Phan, N. H. Lovell, and T. N. Do, "Soft microtubule muscle-driven 3-axis skin-stretch haptic devices," *IEEE Access*, vol. 8, pp. 157878–157891, 2020.
- [39] R. W. Colbrunn, G. M. Nelson, and R. D. Quinn, "Modeling of braided pneumatic actuators for robotic control," in *Proc. IEEE/RSJ Int. Conf. Intell. Robots Syst., Expanding Societal Role Robot. the Next Millennium*, vol. 4, Oct. 2001, pp. 1964–1970.
- [40] S. Jensen. (2006). *Importance of Hose*. [Online]. Available: <https://www.powermotiontech.com/technologies/other-technologies/articled/21884115/chapter-3-pipe-tube-and-hose>
- [41] S. Exner, "Experimentelle untersuchung der einfachsten psychischen prozesse," *Archiv für die Gesamte Physiologie des Menschen und der Thiere*, vol. 11, no. 1, pp. 581–602, Dec. 1875.
- [42] I. M. L. C. Vogels, "Detection of temporal delays in visual-haptic interfaces," *Human Factors, J. Human Factors Ergonom. Soc.*, vol. 46, no. 1, pp. 118–134, Mar. 2004.
- [43] M. Paré, H. Carnahan, and A. Smith, "Magnitude estimation of tangential force applied to the fingerpad," *Exp. Brain Res.*, vol. 142, no. 3, pp. 342–348, Feb. 2002.
- [44] W. A. IJsselsteijn, Y. A. De Kort, and K. Poels, "The game experience questionnaire," Hum. Technol. Interact. Ind. Eng. Innov. Sci., Eindhoven, The Netherlands, Academic Rep., 2013.
- [45] S. Sathiyamurthy, M. Lui, E. Kim, and O. Schneider, "Measuring haptic experience: Elaborating the HX model with scale development," in *Proc. IEEE World Haptics Conf. (WHC)*, Jul. 2021, pp. 979–984.
- [46] D. Schmidt, G. Schlee, T. L. Milani, and A. M. C. Germano, "Vertical contact forces affect vibration perception in human hairy skin," *PeerJ*, vol. 11, Sep. 2023, Art. no. e15952.
- [47] A. Wilska, "On the vibrational sensitivity in different regions of the body surface," *Acta Physiologica Scandinavica*, vol. 31, nos. 2–3, pp. 285–289, Feb. 1954.
- [48] S. J. Lederman and R. L. Klatzky, "Haptic perception: A tutorial," *Attention, Perception Psychophysics*, vol. 71, no. 7, pp. 1439–1459, Oct. 2009.
- [49] R. T. Verrillo and G. A. Gescheider, "Perception via the sense of touch," in *Tactile Aids for Hearing Impaired*. Hoboken, NJ, USA: Wiley, 1992, pp. 1–36.



**AHSAN RAZA** received the B.S. degree in computer engineering from the University of Engineering and Technology (UET) Taxila, Taxila, Pakistan, in 2015. He is currently pursuing the Ph.D. degree with the Department of Computer Science and Engineering, Kyung Hee University, South Korea. His research interests include mid-air haptic feedback, haptic actuator design, and psychophysics.



**WASEEM HASSAN** received the B.S. degree in electrical engineering from the National University of Science and Technology (NUST), Pakistan, and the M.S. and Ph.D. degrees in computer science and engineering from Kyung Hee University, Republic of Korea, in 2016 and 2022, respectively. Currently, he is a Postdoctoral Researcher with the Department of Computer Science, University of Copenhagen, Denmark. His research interests include psychophysics, haptic content generation, and novel haptic interfaces.



**SEOKHEE JEON** (Member, IEEE) received the B.S. and Ph.D. degrees in computer science and engineering from the Pohang University of Science and Technology (POSTECH), in 2003 and 2010, respectively. He was a Postdoctoral Research Associate with the Computer Vision Laboratory, ETH Zürich. In 2012, he joined the Department of Computer Engineering, Kyung Hee University, as an Assistant Professor. His research interests include haptic rendering in an augmented reality environment, the applications of haptics technology to medical training, and the usability of augmented reality applications.

...